Solvent-Isotope and pH Effects on Flagellar Rotation in *Escherichia coli*

Xiaobing Chen and Howard C. Berg
Department of Molecular and Cellular Biology, Harvard University, Cambridge, Massachusetts 02138, and Rowland Institute for Science, Cambridge, Massachusetts 02142 USA

ABSTRACT We studied changes in speed of the flagellar rotary motor of *Escherichia coli* when tethered cells or cells carrying small latex spheres on flagellar stubs were shifted from H_2O to D_2O or subjected to changes in external pH. In the high-torque, low-speed regime, solvent isotope effects were found to be small; in the low-torque, high-speed regime, they were large. The boundaries between these regimes were close to those found earlier in measurements of the torque-speed relationship of the flagellar rotary motor (Berg and Turner, 1993, *Biophys. J.* 65:2201–2216; Chen and Berg, 2000, *Biophys. J.*, 78:1036–1041). This observation provides direct evidence that the decline in torque at high speed is due primarily to limits in rates of proton transfer. However, variations of speed (and torque) with shifts of external pH (from 4.7 to 8.8) were small for both regimes. Therefore, rates of proton transfer are not very dependent on external pH.

INTRODUCTION

Flagellated bacteria swim by rotating helical filaments driven by motors embedded in the cell wall and cytoplasmic membrane (Macnab, 1996; Berry and Armitage, 1999). As one of the systems that demonstrated Mitchell's chemiosmotic hypothesis (Mitchell, 1961; see Harold and Maloney, 1996), the energy source for motility is the proton electrochemical potential: proton charge times protonmotive force (Larsen et al., 1974; Manson et al., 1977; Matsuura et al., 1977). The rotation rate is proportional to the transmembrane proton flux (Meister et al., 1987). Some species of bacteria are powered, instead, by sodium ions (see, for example, Kojima et al., 1999a,b). Detailed mechanisms of torque generation are not yet understood; however, a number of things are known about motor hardware. MotA and MotB are thought to constitute elements of the stator, with charged residues on a cytoplasmic domain of MotA interacting with a complementary set of charged residues on the C-terminal domain of FliG, an element at the periphery of the rotor (Lloyd and Blair, 1997; Zhou and Blair, 1997; Zhou et al., 1998). The structure of this domain is now known in atomic detail (Lloyd et al., 1999). Transmembrane domains of MotA and MotB constitute proton-conducting channels (Sharp et al., 1995a,b).

As an essential window on flagellar motor function, the output torque was determined as a function of speed by two independent methods (Berg and Turner, 1993; Chen and Berg, 2000). Two dynamic regimes were found: one at lower speeds, in which the torque is approximately constant (torque declines slightly with speed), and another at higher speeds, in which the torque declines rapidly. In the low-speed regime, the torque is independent of temperature; in the high-speed regime, it is strongly dependent upon temperature. The absence of both temperature and solvent-isotope effects in the low-speed regime was noted earlier with tethered cells of artificially energized *Streptococcus* (Khan and Berg, 1983). Their presence in the high-speed regime was noted earlier with swimming cells of *Streptococcus*, *Escherichia coli,* and *Salmonella typhimurium* (Lowe et al., 1987; Meister et al., 1987; Blair and Berg, 1990).

Here we report studies of solvent-isotope and pH effects made with motors of cells of *E. coli* operating over a wide dynamic range, comparing results obtained in the low- and high-speed regimes.

MATERIALS AND METHODS

Most of the procedures were described previously (Chen and Berg, 2000). Cells were from strain KAF95, which rotates its motors exclusively counterclockwise and has sticky flagellar filaments. Polystyrene latex spheres (0.36-μm diameter, 2.6% solids) were from Polysciences (Warrington, PA). D_2O (99%) was from Aldrich. The motility medium in H_2O was 10 mM K_2HPO_4/KH_2PO_4, 70 mM NaCl, 0.1 mM EDTA (pH 7.0). A buffer of identical ionic composition was made in D_2O (pD 7.5). pD was measured with a pH meter by adding 0.44 units to the reading (Schowen, 1977). Viscosities of D_2O media were measured at 22.7°C, 17.7°C, and 15.8°C with a Cannon-Ubbelhode capillary viscometer (Cannon Instrument Co., State College, PA), yielding 1.17, 1.33, and 1.41 cp, respectively. The corresponding values for H_2O media were 0.986, 1.08, and 1.14 cp, respectively (Chen and Berg, 2000). This gives a mean ratio of viscosity $D_2O/H_2O = 1.22$, equal to the value found earlier (Khan and Berg, 1983). Media in H_2O at other pHs were prepared either by varying the proportion of KH_2PO_4 and K_2HPO_4 or by titrating the medium of pH 7.0 with 1 M NaOH or 1 M HCl. The first approach differed from the second in that no extra ionic species were introduced; however, K^+ concentrations varied with pH. We checked to see whether these differences had any effect on motility by supplementing the pH 7 medium with different concentrations of K_2HPO_4/KH_2PO_4 (pH 7.0), but no significant changes were detected. As before, exchanges of fluid were made in a temperature-controlled flow cell.

The isotope experiments were conducted by monitoring the rotation rate of tethered cells or of latex spheres on flagellar stubs. The technique for attaching spheres to stubs, described in detail previously (Chen and Berg, 2000), involves the attachment of cells to a silanized coverslip, followed by

Received for publication 8 November 1999 and in final form 7 February 2000.

Address reprint requests to Dr. Howard C. Berg, Department of Molecular and Cellular Biology, Harvard University, 16 Divinity Ave., Cambridge, MA 02138. Tel.: 617-495-0924; Fax: 617-496-1114; E-mail: hberg@biosun.harvard.edu.

0006-3495/00/05/2280/05 $2.00

the addition of a suspension of spheres. Some cells tether rather than attach rigidly, and some spheres stick to flagellar stubs as aggregates. This makes it possible, in a single setup, for one to find motors spinning over a wide range of speeds. The speed of a given motor was measured in H_2O medium (pH 7.0) (Chen and Berg, 2000) and then in D_2O medium (pD 7.5) and then again in H_2O medium, or the other way around. Normally, 1–2 min was required after each exchange to allow the speed to settle down to a new steady-state value. Usually, the initial and final speeds (in the same medium) were the same; if not, another motor was selected. When experiments were carried out at lower temperatures, 10–15 min was allowed after each exchange to ensure temperature equilibration. The pH shift experiments were all conducted at 22.7°C, and ~3 min was allowed for equilibration. Here we explored a series of pHs (typically, five or six per motor, including pH 7.0), visiting the same pH two or three times.

Observations of the speeds of rotation of tethered cells and of latex spheres on flagellar stubs were made in a weak optical trap by back-focal-plane interferometry, as described previously (Chen and Berg, 2000). The trap was too weak to significantly perturb motor rotation.

RESULTS

Motor rotation in H_2O and D_2O

Motor speeds in H_2O medium at pH 7.0 were compared to motor speeds in D_2O medium at pD 7.5, following the method of Khan and Berg (1983). This compensates for the upward shift in internal pH resulting from changes in the pK_a of weak acids and bases, which are higher in D_2O than in H_2O (Schowen, 1977). The torque exerted by a motor spinning an inert object in a medium of viscosity η is $T = b\eta\omega$, where $b\eta$ is the rotational frictional drag coefficient, and ω is the angular velocity ($2\pi\nu$, where ν is the rotational speed in Hz). Because we compared the same motor spinning the same object in D_2O and H_2O, the geometrical factor b remains the same, and $T_D/T_H = (\eta_D\nu_D)/(\eta_H\nu_H)$. The ratio of viscosities is known (1.22), so $T_D/T_H = 1.22\ \nu_D/\nu_H$. This quantity is plotted in Fig. 1 as a function of ν_H, the speed in H_2O. For convenience, fits to these data were made by two linear regressions by an iterative procedure, as described previously (Chen and Berg, 2000). The point of intersection between the two regression lines defines a "knee speed," which distinguishes a low-speed regime, in which the torque (or torque ratio) is approximately constant, from a high-speed regime, in which the torque (or torque ratio) declines rapidly. The "zero-torque" speed is deduced by linear extrapolation of the second regression line. The relative torque curves have approximately the same domain structure as the torque-speed curves, as summarized in Table 1. They also have the same shape and temperature dependence. This provides direct evidence that the decline in torque at high speed observed in the torque-speed relationship is due primarily to limits in rates of proton transfer.

The intercepts of the regression lines at stall ($\nu_H = 0$) at 22.7°C and 15.8°C (Fig. 1) are 0.93 ± 0.03 and 0.85 ± 0.05, respectively. At stall, the efficiencies of energy conversion with the two isotopes should be the same, so these numbers indicate that the deuteromotive force (Δp_D) is slightly smaller than the protonmotive force (Δp_H), presumably because rates of respiration are smaller in D_2O than in H_2O.

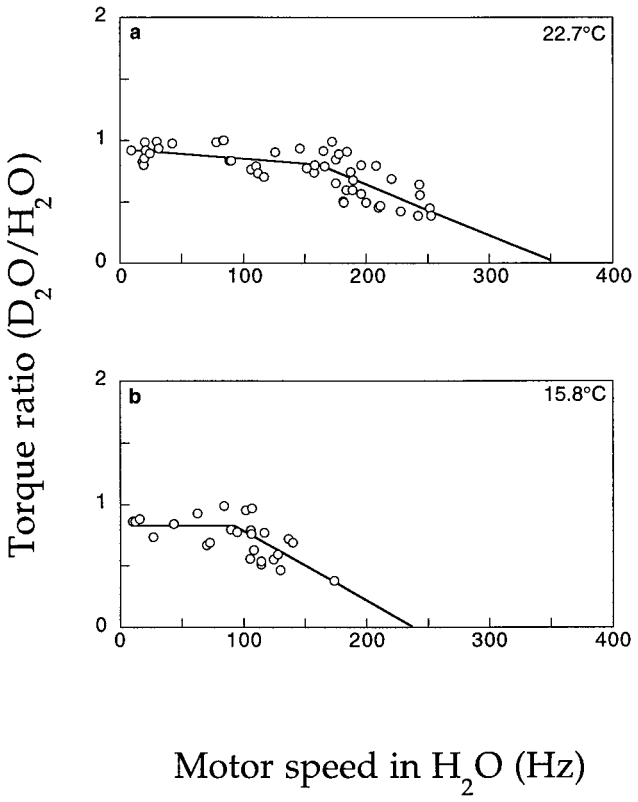

FIGURE 1 Torque in D_2O relative to that in H_2O plotted as a function of speed in H_2O for (*a*) 50 cells at 22.7°C and (*b*) 27 cells at 15.8°C. The lines are two linear regressions below and above the knee speed, respectively, at either temperature.

Motor rotation at different external pH

We compared motor speeds in H_2O medium at pH 7.0 with speeds in H_2O medium at other pHs, ranging from 4.7 to

TABLE 1 Comparison of knee speeds and zero-torque speeds deduced from isotope effects with those obtained previously from measurements of the torque-speed relationship

	Knee speed* (Hz) from		Zero-torque speed† (Hz) from	
Temperature (°C)	Isotope effects	Torque speed	Isotope effects	Torque speed
22.7	162 ± 62 (27, 26)	175 ± 56 (93, 52)	354 ± 99 (26)	350 ± 74 (52)
15.8	92 ± 42 (13, 19)	80 ± 30 (15, 16)	238 ± 76 (19)	180 ± 41 (16)

*The knee speed is obtained from the intersection of two linear regressions. The numbers reported are the mean ± SD (number of data points for each regression).

†The zero-torque speed is obtained from extrapolation of the linear regression for the high-speed data. The numbers reported are the mean ± SD (number of data points for the high-speed regression).

8.8. For a given motor, we normalized the results for each exposure to the mean value of the speeds found at pH 7.0. The results are shown in Fig. 2 for all of the cells studied (Fig. 2 *a*), for the subset with speeds below the knee speed (~175 Hz, Fig. 2 *b*), and for the subset with speeds above the knee speed (Fig. 2 *c*). There was essentially no difference. Given the scatter in the data and the minimal curvature, we simply made linear regressions, shown by the solid lines. These show a general downward trend, with a speed at pH 8.0 roughly 88% of that at pH 5.0. A rough estimate of the difference in behavior in the low-speed and high-speed regimes (Fig. 2, *b* and *c*, respectively) can be found by binning the data and comparing means and standard errors.

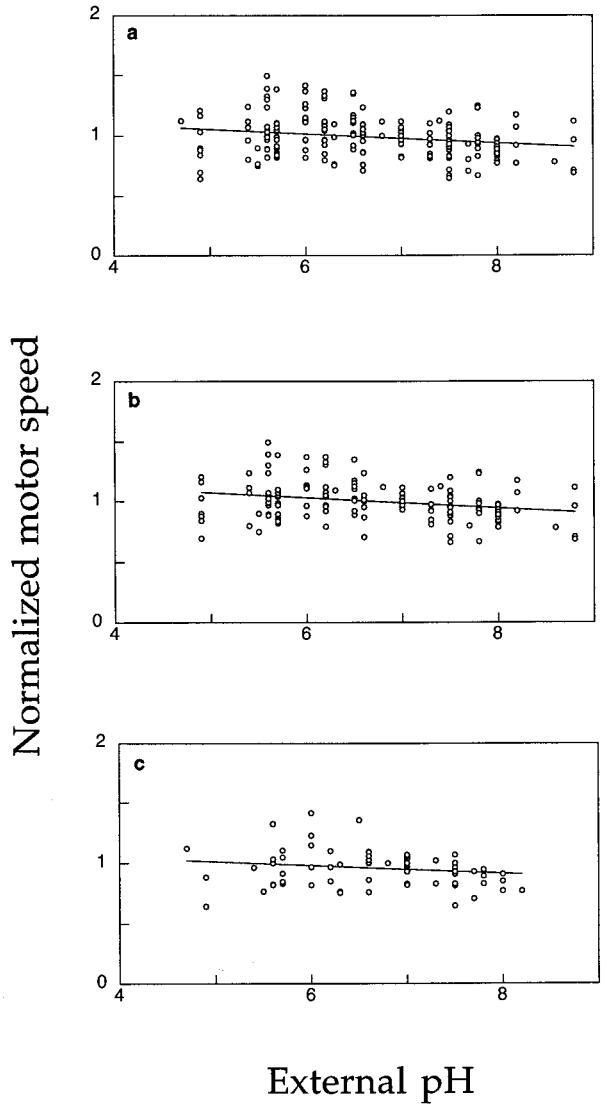

FIGURE 2 Normalized speed as a function of external pH at 22.7°C for (*a*) a set of 50 cells ranging in speed from 17.1 Hz to 257.4 Hz; (*b*) a subset of 30 cells ranging in speed from 17.1 Hz to 175.0 Hz (approximately the knee speed); and (*c*) a subset of 20 cells ranging in speed from 181.1 Hz to 257.4 Hz. The lines are linear regressions.

For Fig. 2 *b*, these values for the pH ranges <6, between 6 and 7, and >7 are 1.02 ± 0.18 (41), 1.03 ± 0.11 (85), and 0.94 ± 0.13 (57). For Fig. 2 *c*, they are 0.94 ± 0.17 (15), 1.01 ± 0.13 (44), and 0.87 ± 0.11 (19). Given the similarity in the data at different speed regimes, it is evident that the torque-speed curves have the same general shape at different external pH levels.

DISCUSSION

Deuterium isotope effects

Solvent isotope effects were relatively small at speeds below the knee speed but relatively large at speeds above the knee speed (Fig. 1). These curves have the same domain boundaries (Table 1), the same shapes, and the same temperature dependence as those determined earlier for the torque-speed relationship (Berg and Turner, 1993; Chen and Berg, 2000). This is exactly as one would expect if the decline in torque at high speed is due to limits in rates of proton transfer or, more specifically, to limits in rates of proton dissociation. At low speeds, the motor appears to operate close to equilibrium, in a domain where rates of proton transfer or of movements of mechanical parts are not limiting. Data obtained previously with tethered cells are consistent with a model in which a fixed number of protons, working near unit efficiency, carry the motor through each revolution (Meister et al., 1987; Fung and Berg, 1995), i.e., the motor is tightly coupled. Because there is relatively little change in behavior up to the knee speed, it is reasonable to assume that the motor continues to operate in this mode up to that point (Chen and Berg, 2000). If the motor remains tightly coupled at speeds higher than the knee speed, the energy conversion efficiency must decline.

To see this quantitatively, consider the motor efficiency α = (power output)/(power input) = $T\omega/ef\Delta p$, where T is torque, ω is angular velocity ($2\pi\nu$), e is proton charge, f is proton flux (protons/s), and Δp is protonmotive force. If we assume tight coupling, $f = n\omega/2\pi$, where n is the number of protons per revolution, so $\alpha = 2\pi T/en\Delta p$. Given $T = b\eta\omega$ (see Results), we get $\alpha = (4\pi^2 b/en)(\eta\nu/\Delta p)$. The parameters in the first set of parentheses should be the same in D_2O as in H_2O. So $\alpha_D/\alpha_H = (\eta_D\nu_D/\eta_H\nu_H)(\Delta p_H/\Delta p_D)$, or $(\eta_D\nu_D/\eta_H\nu_H) = (\alpha_D/\alpha_H)(\Delta p_D/\Delta p_H)$. The quantity on the left in the latter expression, the torque in D_2O relative to that in H_2O, is plotted as a function of ν_H in Fig. 1. If one starts in H_2O at a relatively low speed and shifts to D_2O, the efficiency remains close to 1. If one starts in H_2O at a relatively high speed and shifts to D_2O, the efficiency drops below 1. If one starts in H_2O at a speed at which the efficiency already is below 1 and shifts to D_2O, the efficiency becomes even smaller. A proton dissociation step that is rate limiting in H_2O should be even more so in D_2O.

The flagella of swimming cells appear to exert less torque after shifts to D_2O (Lowe et al., 1987; Meister et al., 1987;

Blair and Berg, 1990). The present work supports that analysis and extends it to a wider dynamic range. In earlier studies with tethered cells of *Streptococcus*, in which the transmembrane potential was clamped by diffusion of potassium, the torque ratio was 0.99 ± 0.02 (Khan and Berg, 1983). This reinforces our belief that the lower value for the torque ratio near stall that is evident in Fig. 1 is due to the fact that Δp_D is slightly less than Δp_H. In earlier work with tethered cells of *E. coli*, this difference was not detected (Blair and Berg, 1990).

pH effects

Speed was nearly independent of external pH from pH 4.7 to pH 8.8, and this was true in both the low- and high-speed regimes (Fig. 2). The decline evident in the figure occurred at a rate somewhat lower than expected, assuming that speed is proportional to Δp_H. Cells of *E. coli* grown aerobically and studied in nongrowth medium maintain homeostasis of internal pH (Padan and Schuldiner, 1987). This is true even for cells grown at different external pHs (Navon et al., 1977). The intracellular pH of *E. coli* is ~7.5, as measured in membrane vesicles (Ramos et al., 1976) or with microelectrodes in giant cells (Felle et al., 1980), and ~7.6, as measured by ^{31}P NMR (Navon et al., 1977; Slonczewski et al., 1981). As the extracellular pH is varied, for example from 5 to 8, the contribution to the protonmotive force from the pH gradient decreases, while the transmembrane electrical potential increases. The net effect is that the protonmotive force declines. So if the rotation rate is proportional to the protonmotive force, we would expect it to decline in a similar manner. The normalized speed dropped from ~1.1 to 0.9 over the pH range 5.0 to 8.0 (Fig. 2). From the data obtained with giant cells (Felle et al., 1980), for example, we would expect the normalized speed to drop from ~1.3 to 0.8.

The more intriguing finding is that the results do not depend on initial speed. That is, a motor operating at high speed and low efficiency is no more susceptible to changes in external pH than one operating at low speed and high efficiency. At high speed, the rate-limiting steps, which involve proton transfer, are not sensitive to changes in external pH, at least over the range 4.7–8.8.

The dependence of speed on external pH has been studied before. The swimming speed of *E. coli* was measured from pH 6 to 7.6, and changes were not detected (Blair and Berg, 1990). With glycolyzing *Streptococcus* (initially at pH 7.5) the pH dependence is bell-shaped, with a maximum near 7. In a study of stalled or freely rotating tethered cells, the torque fell by a factor of ~0.8 at both pH 5.5 and pH 8.0, and by a factor of ~0.4 at pH 9.5 (Meister and Berg, 1987). In a study of tethered or swimming cells, a similar decline was observed at high pH but not at low pH, although the latter shifts were limited to pH 6.5 (Khan et al., 1990). At pH 6.5, tethered cells sped up by a factor of ~1.2, but swimming cells did not. The largest variations in speed with external pH have been observed with metabolizing cells of *Bacillus subtilis* (Shioi et al., 1980). For swimming cells, the dependence is bell-shaped, with a maximum near pH 7, but it drops precipitously below 6 and above 8, by a factor of ~0.5 at pH 5.5 and pH 8.8. All of these organisms maintain pH homeostasis. Both *E. coli* and *B. subtilis* adjust their membrane potential to compensate for changes in Δp_H. *Streptococcus*, which fails to respire, does not (Khan et al., 1990).

Voltage-gated proton channels

In experiments on the torque-speed relationship made by electrorotation (Berg and Turner, 1993), the torque falls linearly from the knee through zero (as in the extrapolation in Fig. 1) and into a regime in which torque changes sign and the motor acts as a brake. At zero torque, the motor does no external work. In that limit, the speed might still be set by the time required for a torque-generating element to execute its mechanochemical cycle. Alternatively, it might be set by the conductance of the channel that delivers protons to that element. Given this possibility, it is intriguing to note that mammalian voltage-gated proton channels exhibit a number of properties similar to those observed when the *E. coli* flagellar motor operates at low torque. The conductance is low and the temperature dependence is high ($Q_{10} \approx 2.8$ at >20°C; DeCoursey and Cherny, 1998)—the motor knee and zero-torque speeds exhibit a Q_{10} of ~3 (Chen and Berg, 2000)—deuterium solvent isotope effects are large (H_2O/D_2O flux ratio ≈ 1.9; DeCoursey and Cherny, 1997), and the dependence on pH (internal or external) is low (DeCoursey and Cherny, 1996). In all of the motor experiments that have been conducted thus far, the channel and the torque-generating element are in series. In the limit of tight coupling, the currents that flow through one also flow through the other. Is it possible to purify a MotA, MotB complex with an open channel and study its properties via patch clamp? Might the channel conductance be so low as to be rate limiting?

We thank Will Ryu for setting up the optical trap and for his technical assistance during the experiments.

This work was supported by grant AI16478 from the National Institutes of Health and by the Rowland Institute for Science.

REFERENCES

Berg, H. C., and L. Turner. 1993. Torque generated by the flagellar motor of *Escherichia coli. Biophys. J.* 65:2201–2216.

Berry, R. M., and J. P. Armitage. 1999. The bacterial flagellar motor. *Adv. Microb. Physiol.* 41:291–337.

Blair, D. F., and H. C. Berg. 1990. The MotA protein of *E. coli* is a proton-conducting component of the flagellar motor. *Cell.* 60:439–449.

Chen, X., and H. C. Berg. 2000. Torque-speed relationship of the flagellar rotary motor. *Biophys. J.* 78:1036–1041.

DeCoursey, T. E., and V. V. Cherny. 1996. Effects of buffer concentration on voltage-gated H^+ currents: does diffusion limit the conductance? *Biophys. J.* 71:182–193.

DeCoursey, T. E., and V. V. Cherny. 1997. Deuterium isotope effects on permeation and gating of proton channels in rat alveolar epithelium. *J. Gen. Physiol.* 109:415–434.

DeCoursey, T. E., and V. V. Cherny. 1998. Temperature-dependence of voltage-gated H^+ currents in human neutrophils, rat alveolar epithelial cells, and mammalian phagocytes. *J. Gen. Physiol.* 112:503–522.

Felle, H., J. S. Porter, C. L. Slayman, and H. R. Kaback. 1980. Quantitative measurements of membrane potential in *Escherichia coli. Biochemistry.* 19:3585–3590.

Fung, D. C., and H. C. Berg. 1995. Powering the flagellar motor of *Escherichia coli* with an external voltage source. *Nature.* 375:809–812.

Harold, F. M., and P. C. Maloney. 1996. Energy transduction by ion currents. *In Escherichia coli* and *Salmonella*: Cellular and Molecular Biology. F. C. Neidhardt, R. Curtiss, J. L. Ingraham, E. C. C. Lin, K. B. Low, B. Magasanik, W. S. Reznikoff, M. Riley, M. Schaechter, and H. E. Umbarger, editors. American Society for Microbiology, Washington, DC. 283–306.

Khan, S., and H. C. Berg. 1983. Isotope and thermal effects in chemiosmotic coupling to the flagellar motor of *Streptococcus. Cell.* 32: 913–919.

Khan, S., M. Dapice, and I. Humayun. 1990. Energy transduction in the bacterial flagellar motor: effects of load and pH. *Biophys. J.* 57: 779–796.

Kojima, S., Y. Asai, T. Atsumi, I. Kawagishi, and M. Homma. 1999a. Na^+-driven flagellar motor resistant to phenamil, an amiloride analogue, caused by mutations in putative channel components. *J. Mol. Biol.* 285:1537–1547.

Kojima, S., K. Yamamoto, I. Kawagishi, and M. Homma. 1999b. The polar flagellar motor of *Vibrio cholerae* is driven by an Na^+ motive force. *J. Bacteriol.* 181:1927–1930.

Larsen, S. H., J. Adler, J. J. Gargus, and R. W. Hogg. 1974. Chemomechanical coupling without ATP: the source of energy for motility and chemotaxis in bacteria. *Proc. Nat. Acad. Sci. USA.* 71:1239–1243.

Lloyd, S. A., and D. F. Blair. 1997. Charged residues of the rotor protein FliG essential for torque generation in the flagellar motor of *Escherichia coli. J. Mol. Biol.* 266:733–744.

Lloyd, S. A., F. G. Whitby, D. F. Blair, and C. P. Hill. 1999. Structure of the C-terminal domain of FliG, a component of the rotor in the bacterial flagellar motor. *Nature.* 400:472–475.

Lowe, G., M. Meister, and H. C. Berg. 1987. Rapid rotation of flagellar bundles in swimming bacteria. *Nature.* 325:637–640.

Macnab, R. M. 1996. Flagella and motility. *In Escherichia coli* and *Salmonella*: Cellular and Molecular Biology. F. C. Neidhardt, R. Curtiss, J. L. Ingraham, E. C. C. Lin, K. B. Low, B. Magasanik, W. S. Reznikoff, M. Riley, M. Schaechter, and H. E. Umbarger, editors. American Society for Microbiology, Washington, DC. 123–145.

Manson, M. D., P. Tedesco, H. C. Berg, F. M. Harold, and C. van der Drift. 1977. A protonmotive force drives bacterial flagella. *Proc. Natl. Acad. Sci. USA.* 74:3060–3064.

Matsuura, S., J.-I. Shioi, and Y. Imae. 1977. Motility in *Bacillus subtilis* driven by an artificial protonmotive force. *FEBS Lett.* 82:187–190.

Meister, M., and H. C. Berg. 1987. The stall torque of the bacterial flagellar motor. *Biophys. J.* 52:413–419.

Meister, M., G. Lowe, and H. C. Berg. 1987. The proton flux through the bacterial flagellar motor. *Cell.* 49:643–650.

Mitchell, P. 1961. Coupling of phosphorylation to electron and hydrogen transfer by a chemiosmotic type of mechanism. *Nature.* 191:144–148.

Navon, G., S. Ogawa, R. G. Shulman, and T. Yamane. 1977. High-resolution ^{31}P nuclear magnetic resonance studies of metabolism in aerobic *Escherichia coli* cells. *Proc. Natl. Acad. Sci. USA.* 74:888–891.

Padan, E., and S. Schuldiner. 1987. Intracellular pH and membrane potential as regulators in the prokaryotic cell. *J. Membr. Biol.* 95:189–198.

Ramos, S., S. Schuldiner, and H. R. Kaback. 1976. The electrochemical gradient of protons and its relationship to active transport in *Escherichia coli* membrane vesicles. *Proc. Natl. Acad. Sci. USA.* 73:1892–1896.

Schowen, R. L. 1977. Solvent isotope effects on enzymic reactions. *In* Isotope Effects on Enzyme-Catalyzed Reactions. W. W. Cleland, M. H. O'Leary, and D. B. Northrop, editors. University Park Press, Baltimore, MD. 64–99.

Sharp, L. L., J. Zhou, and D. F. Blair. 1995a. Features of MotA proton channel structure revealed by tryptophan-scanning mutagenesis. *Proc. Natl. Acad. Sci. USA.* 92:7946–7950.

Sharp, L. L., J. Zhou, and D. F. Blair. 1995b. Tryptophan-scanning mutagenesis of Mot B, an integral membrane protein essential for flagellar rotation in *Escherichia coli. Biochemistry.* 34:9166–9171.

Shioi, J.-I., S. Matsuura, and Y. Imae. 1980. Quantitative measurements of protonmotive force and motility in *Bacillus subtilis. J. Bacteriol.* 144: 891–897.

Slonczewski, J. L., B. P. Rosen, J. R. Alger, and R. M. Macnab. 1981. pH homeostasis in *Escherichia coli*: measurement by ^{31}P nuclear magnetic resonance of methylphosphonate and phosphate. *Proc. Natl. Acad. Sci. USA.* 78:6271–6275.

Zhou, J., and D. F. Blair. 1997. Residues of the cytoplasmic domain of MotA essential for torque generation in the bacterial flagellar motor. *J. Mol. Biol.* 273:428–439.

Zhou, J., S. A. Lloyd, and D. F. Blair. 1998. Electrostatic interactions between rotor and stator in the bacterial flagellar motor. *Proc. Natl. Acad. Sci. USA.* 95:6436–6441.